Regulation of Intracellular Chloride by Cotransporters in Developing Lateral Superior Olive Neurons

Yasuhiro Kakazu,[1,2] Norio Akaike,[1] Soutaro Komiyama,[2] and Junichi Nabekura[1]

Departments of [1]Physiology and [2]Otorhinolaryngology, Faculty of Medicine, Kyushu University, Fukuoka 812–8582, Japan

The regulatory mechanisms of intracellular Cl^- concentration ($[Cl^-]_i$) were investigated in the lateral superior olive (LSO) neurons of various developmental stages by taking advantage of gramicidin perforated patch recording mode, which enables neuronal $[Cl^-]_i$ measurement. Responses to glycine changed from depolarization to hyperpolarization during the second week after birth, resulting from $[Cl^-]_i$ decrease. Furosemide equally altered the $[Cl^-]_i$ of both immature and mature LSO neurons, indicating substantial contributions of furosemide-sensitive intracellular Cl^- regulators; i.e., K^+–Cl^- cotransporter (KCC) and Na^+-K^+-Cl^- cotransporter (NKCC), throughout this early development. Increase of extracellular K^+ concentration and replacement of intracellular K^+ with Cs^+ resulted in $[Cl^-]_i$ elevation at postnatal days 13–15 (P13–P15), but not at P0–P2, indicating that the mechanism of neuronal Cl^- extrusion is sensitive to both furosemide and K^+-gradient and poorly developed in immature LSO neurons. In addition, removal of extracellular Na^+ decreased $[Cl^-]_i$ at P0–P2, suggesting the existence of extracellular Na^+-dependent and furosemide-sensitive Cl^- accumulation in immature LSO neurons. These data show clearly that developmental changes of Cl^- cotransporters alter $[Cl^-]_i$ and are responsible for the switch from the neonatal Cl^- efflux to the mature Cl^- influx in LSO neurons. Such maturational changes in Cl^- cotransporters might have the important functional roles for glycinergic and GABAergic synaptic transmission and the broader implications for LSO and auditory development.

Key words: Cl^--cotransporter; lateral superior olive neurons; development; glycine; intracellular Cl^- concentration; gramicidin perforated patch clamp

The lateral superior olive (LSO) is the first auditory center that processes differences in the sound level between the two ears (Wu and Kelly, 1992; Sanes, 1993). The LSO receives glutamatergic innervation directly from the ipsilateral cochlea nucleus and glycinergic inputs indirectly from the contralateral cochlea nucleus via the medial nucleus of the trapezoid body (Suneja et al., 1995; Vater, 1995). Removal of glycinergic inputs before the onset of hearing results in a hypertrophic response in the LSO (Sanes and Chokshi, 1992), suggesting that the glycinergic transmission may play an important role in the development of LSO.

Several studies have recently shown that GABA and glycine evoke membrane depolarization mediated by the efflux of Cl^- in immature animals, resulting from a high intracellular Cl^- concentration ($[Cl^-]_i$) in CNS during early postnatal life (Luhmann and Prince, 1991; Chen et al., 1996; Backus et al., 1998). This depolarization activates voltage-dependent Ca^{2+} channels and reduces voltage-dependent Mg^{2+} block of NMDA channels, resulting in Ca^{2+} influx (Obrietan and van den Pol, 1997; Leinekugel et al., 1997; Flint et al., 1998). This increase of intracellular Ca^{2+} concentration ($[Ca^{2+}]_i$) plays an important role in neuronal development (LoTurco et al., 1995; Ikeda et al., 1997; Kirsch and Betz, 1998). With neuronal maturation, in turn, $[Cl^-]_i$ becomes lower, which results in the hyperpolarization by GABA and glycine. The high and low $[Cl^-]_i$ in immature and in mature neurons cannot be explained simply by a passive Cl^- distribution (Alvarez-Leefmans, 1990). Although the developmental change in $[Cl^-]_i$ might be caused by alterations of active mechanisms such as Na^+–K^+–Cl^- (NKCC) and K^+–Cl^- (KCC) cotransporters, Cl^-–HCO_3^- exchanger, Cl^-–ATPase and Na^+-dependent Cl^-–HCO_3^- exchanger (Kaila, 1994), the exact mechanism has not yet been identified.

In the present study, the functional involvement of NKCC and KCC in $[Cl^-]_i$ control was examined in developing rat LSO neurons between postnatal day 0 (P0) and P15. KCC cotransports K^+ and Cl^- electroneutrally (1:1) and has been identified to neurons (Payne et al., 1996). Using K^+ gradient produced by Na^+-K^+-ATPase, KCC expels Cl^- with K^+ out of the neuron (Alvarez-Leefmans, 1990). On the other hand, NKCC, which carries Na^+, K^+, and Cl^- simultaneously and electroneutrally (1:1:2) in the same direction, has been well characterized in a wide variety of non-nervous (Haas, 1994) and nervous tissue (Ballanyi and Grafe, 1985; Rohrbough and Spizter, 1996). NKCC is thought to contribute to $[Cl^-]_i$ increase. However, its functional role in mammalian CNS is still unknown. Furthermore, it is difficult to directly evaluate the functional roles of NKCC and KCC by using traditional electrophysiological methods such as conventional nystatin and amphotericin B perforated patch recordings because the net ion movements by KCC and NKCC are electrically neutral and because of the internal dialysis of the cell by the recording pipette in these configurations (Ebihara et al., 1995). For this reason, we used a gramicidin perforated patch recording mode, which allows electrical recording without disruption of native $[Cl^-]_i$ (Akaike, 1997).

Received Nov. 3, 1998; revised Jan. 19, 1999; accepted Jan. 26, 1999.

This work was supported by Grant-in-Aids (Nos. 10156231 and 09670046 to J.N., and Nos. 10470009 and 10044301 to N.A.) from the Ministry of Education, Science and Culture, Japan. We thank Profs. M. Andressen and K. Kaila for critical reading of this manuscript.

Correspondence should be addressed to Dr. J. Nabekura, Department of Physiology, Faculty of Medicine, Kyushu University, Fukuoka 812–82, Japan.

Table 1. External solutions used for electrical recordings

	Extracellular solutions										
	NaCl	KCl	$MgCl_2$	$CaCl_2$	HEPES	Glucose	pH	α[Cl^-]	Mannitol	NMDG-Cl	mOsm/kg
Standard	150	5	1	2	10	10	7.4	114.5			317
20 K^+	135	20	1	2	10	10	7.4	122.5			322
NMDG	0	5	1	2	10	10	7.4	94.2		150	324
Modified standard	110	5	1	2	10	10	7.4	95.6	80		326

MATERIALS AND METHODS

Dissociated LSO neurons. The experimental protocol was approved by the Ethics Review Committee for Animal Experimentation of our institution. Wistar rats aged P0–P15 (either sex) were decapitated under anesthesia with pentobarbitone sodium (55 mg/kg, i.p.), and 300 μm transverse slices of the brain, including the LSO, were prepared with a microslicer (model DTK-1000, D.S.K.; model VT-1000S, Leica, Nussloch, Germany). The slices were incubated for 10–20 min in incubation solution saturated with 95% O_2 and 5% CO_2 gas mixture at room temperature. They were then treated with pronase (1 mg/6–20 ml) at 31°C for 20–45 min and subsequently with thermolysin (1 mg/6–20 ml) under the same conditions. The LSO region was identified on both sides under a binocular microscope (model SMZ-1, Nikon) and punched out from the slice using an electrolytically polished injection needle. The micropunched pieces were triturated mechanically with fine glass pipettes in the standard solution under a phase-contrast microscope (model TMS-1, Nikon). The dissociated LSO neurons adhered to the bottom of the Petri dish within 30 min. Neurons having their original morphological features, such as the dendritic processes, were used in the present experiments.

Solutions. The incubation solution for slices contained (in mM): NaCl, 124; KCl, 5; KH_2PO_4, 1.2; $MgSO_4$, 1.3; $CaCl_2$, 2.4; glucose, 10; and $NaHCO_3$, 24, pH 7.45, with 95% O_2 and 5% CO_2. External solutions used for electrical recordings are listed in Table 1. For Na^+-free extracellular solution (NMDG solution), Na^+ was replaced with *N*-methyl-D-glucosamine (NMDG)-OH, which was first dissolved in water and titrated with HCl at pH 7.0 ± 0.1. Active Cl^- concentration in the extracellular solutions (α[Cl^-]$_o$) were measured by Cl^--sensitive electrode fabricated using a liquid ion exchanger (WPI model IE-170) according to the method reported by Komune et al. (1993). The osmolarity of each solution was measured by the osmometer (model OM802; Vogel). The patch pipette solution for gramicidin perforated patch recording contained (in mM) KCl, 150 and HEPES, 10. For the Cs^+-containing pipette, KCl was simply substituted with CsCl. The patch pipette solution for nystatin perforated patch recording contained (in mM): KCl, 50; K-gluconate, 100; and HEPES, 10. All pipette solutions were buffered to pH 7.2 with Tris-OH. Gramicidin was first dissolved in methanol to prepare a stock solution of 10 mg/ml and then diluted to a final concentration of 100 μg/ml in the pipette solutions. The gramicidin-containing solution was prepared just before the experiment. When nystatin perforated patch mode was used, the 10 mg/ml stock solution of nystatin (Akaike and Harata, 1994) was diluted to a final concentration of 400 μg/ml in the pipette solutions.

Electrophysiological measurements. Ionic currents and voltages were measured with a patch-clamp amplifier (EPC-7; List Electronic), low-pass filtered at 1 kHz (FV-665; NF Electronic Instruments), and monitored on both an oscilloscope (HS-5100A; Iwatsu) and a pen recorder (Recti-Horiz-8K21; Nihondenki San-ei). In ramp experiments, 3×10^{-7} M tetrodotoxin (TTX) and 10^{-5} M $LaCl_3$ were added to the extracellular solutions. Ramp voltage steps were applied by using a function generator (VP-7402A; National). Data were also simultaneously recorded on a digital FM tape recorder (RD-120TE; TEAC). Patch pipettes were constructed of glass capillary tubes with an outer diameter of 1.5 mm prepared using a vertical puller (PB-7; Narishige, Tokyo, Japan). The tip resistance of the electrodes was 4–8 MΩ. The junction potential between the patch pipettes and bath solution was nulled before gigaohm seal formation. After establishing contact with the cell surface, a gigaohm seal was established by applying gentle suction to the patch pipette interior. After the cell-attached configuration had been attained, patch pipette potential was held at −50 mV, and −10 mV hyperpolarizing step pulses with 300 msec duration were periodically delivered to monitor the access resistance. In the gramicidin perforated patch recording mode, the access resistance reached a steady level of 20 MΩ within 40 min after making the GΩ seal. In the conventional whole-cell configuration after rupturing gramicidin perforated patch membrane by adding greater negative pressure to the pipette interior, E_{Gly} moved to ~0 mV (+4.7 mV by Nernst equation using active Cl^- concentration in standard solution and 150 mM KCl pipette solution). Thus, the difference in E_{Gly} between gramicidin perforated patch and conventional whole-cell recordings is a good indicator for monitoring the recording condition. In all experiments, 75–80% series resistance compensation was used. All experiments were performed at room temperature (22–26°C).

Drugs. Rapid "square-wave" change of external solution was performed with the "Y-tube" method described previously (Nakagawa et al., 1990). Using this method, the external solution could be completely exchanged within 20 msec. Drugs used in the experiments were gramicidin D, thermolysin, ethacrynic acid (Sigma, St. Louis, MO), pronase (Calbiochem, San Diego, CA), glycine (Kanto, Tokyo, Japan), furosemide (Tokyo Kasei, Tokyo, Japan), and TTX (Sankyo, Tokyo, Japan). Furosemide was dissolved in dimethyl sulfoxide (DMSO) at a concentration of 1 M for the preparation of a stock solution, and the final DMSO concentration in the experiments did not exceed 0.1%.

Statistical analysis. Data were expressed as mean ± SEM. Differences between groups were analyzed for statistical significance using the Student's *t* test. A p value <0.05 denoted the presence of a statistically significant difference.

RESULTS

Glycine responses in developing LSO neurons

Either conventional "open" patch whole-cell recording leads to a rapid equilibration of intracellular cytoplasm with the pipette solution. Perforated patch recordings using nystatin or amphotericin B while limiting dialysis nevertheless alter [Cl^-]$_i$ because of their Cl^- permeability (Ebihara et al., 1995; Rhee et al., 1994). Thus, in the present study, we used the gramicidin for perforated patch recording on LSO neurons acutely dissociated from rats aged between P0 and P15, because it allows selective permeation to monovalent cations without fluxing any anions (Ebihara et al., 1995).

To observe the developmental change in glycine responses, the rats were divided into three age groups (P0–P2, P6–P8, and P13–P15). In the current-clamp mode, 3×10^{-5} M glycine induced a depolarization in 4 of 5 isolated LSO neurons at P0–P2 (Fig. 1A_a) and a hyperpolarization in four of four neurons at P13–P15 (Fig. 1A_b) in the standard extracellular solution. The glycine-induced depolarization was associated with action potentials. Both the glycine-induced depolarization ($n = 2$) and hyperpolarization ($n = 2$) were completely blocked by 10^{-6} M strychnine, suggesting that both responses were mediated by strychnine-sensitive glycine receptors. During voltage-clamp at a V_H of −50 mV, 3×10^{-5} M glycine elicited inward currents at P0–P2 (20 of 37, Fig. 1B_a) and outward currents at P13–P15 (37 of 37, Fig. 1B_b) in the standard extracellular solution.

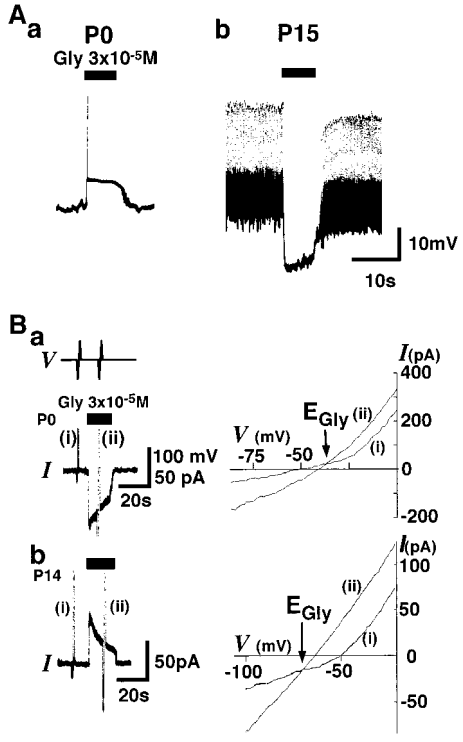

Figure 1. Developmental changes in glycine responses in isolated LSO neurons. A_a, At P0, 3×10^{-5} M glycine (*Gly*, *closed bars*) induced depolarization associated with an action potential (*vertical line*) in a current-clamp mode under gramicidin perforated patch recording configuration. A_b, At P15, glycine induced a hyperpolarization, leading to the blockage of spontaneous action potentials. Resting membrane potentials (V_{rest}s) were −53 and −60 mV in *a* and *b*, respectively. In the present study, test solutions were applied by the Y-tube method. B_a, *Left*, In a voltage-clamp mode, glycine-induced current (I_{Gly}) at a holding potential (V_H) of −50 mV was inward at P0 (*bottom trace, I*). Transient vertical lines (*i* and *ii*) indicate the current responses to steps in ramp voltage. The experimental protocol for ramp voltage steps from −100 to 0 mV with 2 sec duration was made before and during application of 3×10^{-5} M glycine (*top trace*, *V*). *Right*, Current–voltage relationships obtained from ramp voltage steps (*i* and *ii*). The reversal potential of I_{Gly} (E_{Gly}) indicated by the intersection of *i* and *ii* was −35 mV at P0. B_b, *Left*, Glycine induced an outward current at a V_H of −50 mV at P14. *Right*, E_{Gly} was −70 mV. E_{Gly}s were obtained using the protocol described above.

Developmental changes in reversal potential of glycine responses and $[Cl^-]_i$

The reversal potential of glycine responses (E_{Gly}) was measured by voltage ramps applied before and during 3×10^{-5} M glycine under voltage-clamp conditions (Fig. 1*B*). When the resting membrane potential (V_{rest}) measured in the current-clamp mode was compared with E_{Gly} in each LSO neuron, in >50% of LSO neurons at P0–P2 and P6–P8, E_{Gly} was more depolarized than V_{rest} (Fig. 2). On the other hand, E_{Gly} was more hyperpolarized than V_{rest} in ~90% of LSO neurons at P13–P15 (Fig. 2). Significant differences in the mean values of V_{rest} were observed between P0–P2 and P13–P15 ($p < 0.05$) and between P6–P8 and P13–P15 ($p < 0.05$; Table 2). These findings agree with previous studies showing more depolarized resting membrane potentials in immature than in mature neurons (McCormick and Prince, 1987; Luhmann and Prince, 1991).

In our *in vitro* system, the glycine-induced responses in rat LSO neurons were likely to result from a Cl^- gradient favoring the flux of Cl^- through glycine-operated Cl^- channels, and E_{Gly} was considered to be the Cl^- equilibrium potential, then the intact intracellular Cl^- activity ($a[Cl^-]_i$) could be calculated by the Nernst equation using the E_{Gly} and known extracellular Cl^- activities ($a[Cl^-]_o$; Table 1) for each LSO neuron (Ebihara et al., 1995). The distributions of E_{Gly} and $a[Cl^-]_i$ were skewed at P13~P15 (Fig. 3). Statistically significant differences in $a[Cl^-]_i$ were present between P0–P2 and P13–P15 ($p < 0.01$), and between P6–P8 and P13–P15 ($p < 0.01$; Table 2). These results indicate that glycine switched from an excitatory to an inhibitory neurotransmitter because of a fall in $[Cl^-]_i$ during the second week after birth in LSO neurons.

Regulation of $[Cl^-]_i$ by cation–chloride cotransporters during development

Several studies have demonstrated that KCC and NKCC cotransporters play important roles in the maintenance of $[Cl^-]_i$ in both mature (Thompson and Gähwiler, 1989; Zhang et al., 1991) and immature neurons (Rohrbough and Spitzer, 1996). To examine the functional roles of these cotransporters in maintaining $[Cl^-]_i$ in LSO neurons, we used the following strategies: (1) the *p*-sulfamoylbenzoic acid loop diuretic furosemide is a potent inhibitor of both cotransporters (Thompson and Gähwiler, 1989; Haas, 1994); and (2) activation of KCC and NKCC requires the simultaneous presence of K^+ with Cl^-, and of both Na^+ and K^+ with Cl^-, respectively. The absence of any cation inhibits the activity of these cotransporters (Thompson and Gähwiler, 1989; Haas, 1994). The functional roles of these cotransporters were examined using the recovery to glycine responses and the resulting disruption of $[Cl^-]_i$ by the opening of glycine-operated Cl^- channel.

Effect of furosemide

At P0–P2, the majority of I_{Gly}s exhibited inward currents at a V_H of −50 mV (Fig. 4*A*, *top trace*). In the presence of 1 mM furosemide, the amplitude of I_{Gly} gradually decreased and finally became almost null. At P13–P15, furosemide gradually diminished the outward I_{Gly} at a V_H of −50 mV (Fig. 4*A*, *bottom trace*). These I_{Gly}s suppressed by furosemide reappeared when V_H was changed from −50 mV to a different membrane potential (−30 mV at P0–P2 and −70 mV at P13–P15). Reappearance of I_{Gly}s was also associated with a gradual decrease in the amplitude in the presence of furosemide (Fig. 4*A*). Differences between E_{Gly}s and V_H became less in the presence of furosemide at both ages (Fig. 4*B*). These results indicate that furosemide-sensitive mechanisms, such as KCC and NKCC, play a major role in maintaining $[Cl^-]_i$ in both immature and mature LSO neurons.

In addition to its blocking effect of cotransporters, furosemide also acts as a Cl^- channel blocker on $GABA_A$ receptor-containing α4 and α6 subunits (Korpi and Luddens, 1997). However, this was not the case in furosemide-induced reduction of I_{Gly} because under a nystatin perforated patch recording, in which $[Cl^-]_i$ is equal to Cl^- concentration in the pipette solution ($[Cl^-]_{pipette}$), furosemide had little effects on I_{Gly}s or E_{Gly}s at both P0–P2 and P13–P15 ($n = 4$; data not shown), suggesting that the channel-blocking effect of furosemide on the glycine receptor was unlikely in LSO neurons. Thus, furosemide effectively blocked intracellular Cl^- regulators in both ages.

Effect of extracellular K^+ on $[Cl^-]_i$

A change in extracellular K^+ concentration ($[K^+]_o$) from 5 to 20 mM resulted in a gradual reduction in the amplitude of outward I_{Gly} at a V_H of −50 mV at P13–P15 (Fig. 5*A*, *top trace*). Indeed, in

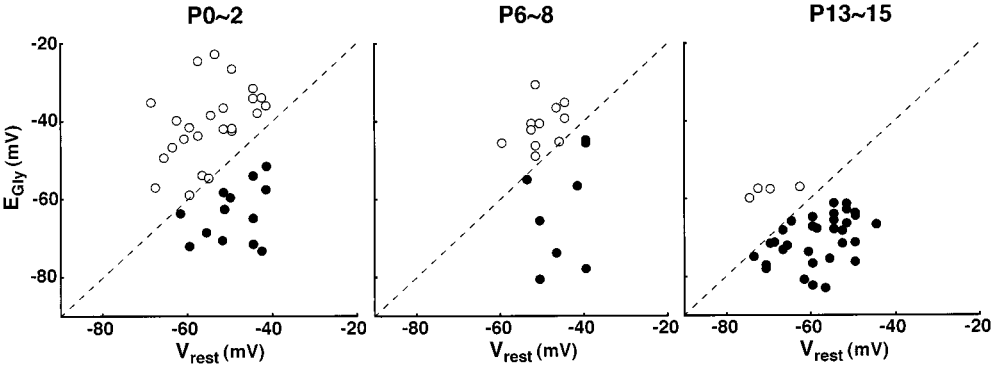

Figure 2. Relationships between V_{rest} and E_{Gly} in developing LSO neurons. E_{Gly} is plotted as a function of V_{rest} in each neuron examined at P0–P2, P6–P8, and P13–P15 (n = 37, 19, and 37, respectively). *Dashed lines* indicate $E_{Gly} = V_{rest}$. *Open* and *closed circles* indicate the neurons with $E_{Gly} > V_{rest}$ and $E_{Gly} < V_{rest}$, respectively. The percentages of LSO neurons with $E_{Gly} > V_{rest}$ are 65, 58, and 11% at P0–P2, P6–P8, and P13–P15, respectively. Note that the number of neurons with $E_{Gly} > V_{rest}$ decreases with maturation.

Table 2. Differences in the mean values of V_{rest}, E_{Gly}, and $\alpha[Cl^-]_i$

	P0–P2 (n = 37)	P6–P8 (n = 19)	P13–P15 (n = 37)
V_{rest}	−53.2 ± 1.3 mV (−41 ~ −70 mV)	−48.5 ± 1.3 mV (−40 ~ −60 mV)	−59.9 ± 1.3 mV (−45 ~ −75 mV)
E_{Gly}	−48.1 ± 2.3 mV (−22.1 ~ −72.7 mV)	−49.5 ± 3.3 mV (−34.6 ~ −80.0 mV)	−68.2 ± 1.2 mV (−56.4 ~ −82.4 mV)
$\alpha[Cl^-]_i$	19.6 ± 1.8 mM (6.4 ~ 47.4 mM)	18.2 ± 1.9 mM (4.8 ~ 34.6 mM)	7.9 ± 0.3 mM (4.3 ~ 12.1 mM)

Mean ± SEM, (), range of values.

20 mM $[K^+]_o$, $\alpha[Cl^-]_i$ calculated from E_{Gly} gradually increased to reach a new value, which was significantly higher than that at 5 mM $[K^+]_o$ at a V_H of −50 mV (Fig. 5*B*; n = 5; $p < 0.01$; paired t test). Unlike furosemide, the outward I_{Gly} changed to an inward one in the presence of 20 mM $[K^+]_o$ at a V_H of −60 mV (Fig. 5*A*, *bottom trace*). In addition, $\alpha[Cl^-]_i$ in 20 mM $[K^+]_o$ at a V_H of −60 mV was similar to that at V_H of −50 mV, which was greater than passive $\alpha[Cl^-]_i$ calculated from V_H and $\alpha[Cl^-]_o$ (10.6 mM at a V_H of −60 mV, Fig. 5*B*). After reversal of $[K^+]_o$ from 20 to 5 mM, $\alpha[Cl^-]_i$ gradually recovered to values similar to that before 20 mM $[K^+]_o$. This result indicates that $[K^+]_o$-dependent $[Cl^-]_i$ regulation, which might be less influenced by the membrane potential, plays an important role in extruding Cl^- at P13–P15. On the other hand, $\alpha[Cl^-]_i$ at P0–P2 was less affected by change in $[K^+]_o$ (n = 4; Fig. 5*B*). These results indicate that $[K^+]_o$-dependent $[Cl^-]_i$ regulation is well developed at P13–P15, but not at P0–P2 in LSO neurons.

Effect of intracellular K^+ on $[Cl^-]_i$

To examine the effect of intracellular K^+ concentration ($[K^+]_i$) on $[Cl^-]_i$, the 150 mM K^+ in the pipette solution ($[K^+]_{pipette}$) was replaced with 150 mM Cs^+ ($[Cs^+]_{pipette}$). Only after the access resistance decreased to <20 MΩ and became stable as confirmed by rectangular pulses from −50 to −60 mV with 300 msec duration, we measured I_{Gly} and E_{Gly}. At P0–P2, $[Cs^+]_{pipette}$ barely influenced the inward I_{Gly} at a V_H of −50 mV (Fig. 6*A*, *top trace*) and $\alpha[Cl^-]_i$ (Fig. 6*B*) throughout recording period. On the other hand, the amplitude of outward I_{Gly} gradually decreased in $[Cs^+]_{pipette}$ in all four neurons examined at P13–P15 (Fig. 6*A*, *bottom trace*). In two of four neurons, I_{Gly} turned inward at a V_H of −50 mV. Furthermore, although the initial values of $\alpha[Cl^-]_i$s in $[Cs^+]_{pipette}$ and $[K^+]_{pipette}$ were similar (Fig. 6*B*, *arrow*), which is consistent with a low resting Cl^- permeability (Thompson and Gähwiler, 1989), $\alpha[Cl^-]_i$ in $[Cs^+]_{pipette}$ gradually reached a significantly high value relative to that in $[K^+]_{pipette}$. These results suggest that $[K^+]_i$-dependent $[Cl^-]_i$ regulation exists at P13–P15, assuming mainly extruding Cl^- out of the cell, but is largely absent at P0–P2. When the results of high $[K^+]_o$ (Fig. 5) and $[Cs^+]_{pipette}$ experiments (Fig. 6) were considered together, the mechanism of Cl^- extrusion, which is sensitive to furosemide as well the K^+-gradient, i.e., KCC, is mainly responsible for the lower $[Cl^-]_i$ in mature LSO neurons. However this Cl^- extrusion mechanism is not well developed at P0–P2.

Effect of extracellular Na^+ on $[Cl^-]_i$

To explore the dependence of $[Cl^-]_i$ regulation on extracellular Na^+ ($[Na^+]_o$), $[Na^+]_o$ was replaced by NMDG. However, simple substitution of 150 mM Na^+ with 150 mM NMDG decreased $\alpha[Cl^-]_o$ by 20 mM, measured by the Cl^--sensitive electrode (Table 1). Indeed, this replacement changed the amplitude of I_{Gly} and shifted E_{Gly} even in nystatin perforated patch recordings (data not shown). To maintain a constant $\alpha[Cl^-]_o$ throughout the experiment, we used a modified standard solution in which 40 mM NaCl in standard solution was substituted with 80 mM mannitol. The osmolarity and $\alpha[Cl^-]_o$ of the modified standard solution were almost equal to those in NMDG solution (Table 1). The amplitudes of I_{Gly} and E_{Gly} measured under a nystatin perforated patch recording, in which $[Cl^-]_i$ was assumed to be equal to $[Cl^-]_{pipette}$, using the modified standard solution was not different to that measured using NMDG solution (n = 3; data not shown).

In gramicidin perforated patch recording, the amplitude of inward I_{Gly} at a V_H of −50 mV gradually decreased after removal of $[Na^+]_o$ at P0–P2 (Fig. 7) but recovered to the initial values after reversal of $[Na^+]_o$ from 0 to 110 mM (n = 4). These results indicate that $[Na^+]_o$-dependent Cl^- accumulation into the cell exists at P0–P2. On the other hand, the effect of removal of $[Na^+]_o$ on $[Cl^-]_i$ was variable at P13–P15 (n = 4). For example, $\alpha[Cl^-]_i$ gradually decreased and then reached a plateau in $[Na^+]_o$-free solution at P13–P15 (n = 2; Fig. 7*B*); $\alpha[Cl^-]_i$ gradually returned to that before 0 mM $[Na^+]_o$. However, in other neurons that exhibited a lower a $\alpha[Cl^-]_i$ in 110 mM $[Na^+]_o$, removal of $[Na^+]_o$ did not affect $\alpha[Cl^-]_o$ (n = 2; Fig. 7*B*). These data indicate that $[Na^+]_o$-dependent Cl^- accumulation plays an important role in $[Cl^-]_i$ regulation at P0–P2 but is variable at P13–P15.

These results indicate that the existence of $[Na^+]_o$-dependent Cl^- accumulation, i.e., NKCC, and lack of K^+ gradient-

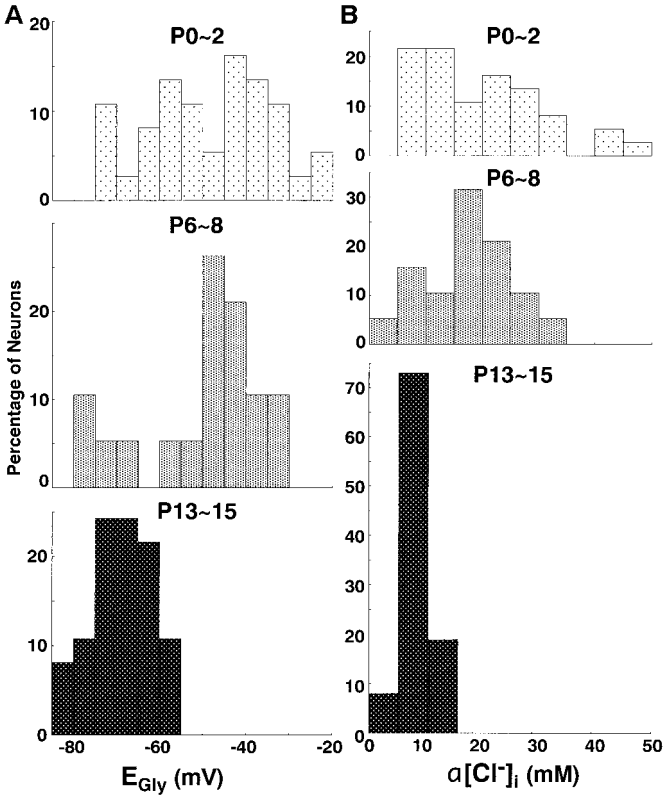

Figure 3. Developmental changes in the active intracellular Cl^- concentration ($\alpha[Cl^-]_i$) in LSO neurons. Histograms of the percentages of LSO neurons are indicated as a function of E_{Gly} (*A*) and $\alpha[Cl^-]_i$ (*B*) at P0–P2, P6–P8, and P13–P15, respectively. LSO neurons examined totaled 37, 19, and 37 at P0–P2, P6–P8, and P13–P15, respectively.

dependent Cl^- extrusion, i.e., KCC, are responsible for the high $[Cl^-]_i$ in immature neurons. Indeed, in LSO neurons at P0, which showed a stable amplitude of inward I_{Gly} at a V_H of −50 mV in the standard extracellular solution, a shift of V_H to −30 mV altered the direction of I_{Gly} to become outward in direction and led to a gradual decrease in the amplitude of the outward I_{Gly}. Finally, the I_{Gly} became almost null (Fig. 8*A*). $\alpha[Cl^-]_i$ increased to the passive $\alpha[Cl^-]_i$ calculated from V_H and $\alpha[Cl^-]_o$ (passive $\alpha[Cl^-]_i$ at a V_H of −30 mV: 34.8 mM, Fig. 8*B*). This finding was compatible with the result that $[Cl^-]_i$ decrease after the efflux of Cl^- through the glycine receptor can be supplied and maintained by Cl^- accumulation mechanism, but $[Cl^-]_i$ increase by the influx of Cl^- through the channels cannot be carried out of the cell because of the lack of Cl^- extrusion mechanism at P0.

DISCUSSION

Developmental changes in glycine responses

Electrophysiological studies indicate that, during early postnatal life, neuronal responses to GABA and glycine, the two major inhibitory neurotransmitters in mature CNS, consist of depolarization rather than hyperpolarization (Luhmann and Prince, 1991; Chen et al., 1996; Backus et al., 1998). Present results showed a variability in E_{Gly}s from one cell to another at each stage of development (Figs. 2, 3), and glycine-induced depolarization was observed in 65% LSO neurons at P0–P2 in the present study (Fig. 2). However, others reported that glycine and electrical stimulation of the glycinergic inputs to LSO depolarized all LSO neurons at P0–P4 (Kandler and Friauf, 1995). The difference in the prevalence of immature LSO neurons with a depolarizing response to glycine might be caused by the following reasons. (1) Because Kandler and Friauf used external solutions containing HCO_3^- and brain slice preparation, depolarization was probably caused by Cl^- efflux as well as HCO_3^- efflux (Staley et al., 1995) and $[K^+]_o$ accumulation (Kaila et al., 1997). However, such mechanisms are unlikely to contribute to glycine-induced depolarizations in the present study, because we used extracellular standard solutions buffered with HEPES, not HCO_3^-, and the dissociated neurons were well superfused in our *in vitro* system. (2) Despite carefully micropunching our specimen within the LSO, we cannot exclude the possibility that some neurons other than those of LSO might be used. (3) Heterogeneous development of neuronal characteristics has been reported in various CNS areas including LSO. The prolonged depolarization mediated by metabotropic glutamatergic receptors is reported in 60% of LSO neurons in immature gerbils (Kotak and Sanes, 1995). A heterogeneous development of NMDA receptor response has been reported in neurons of the nucleus tractus solitarius (Nabekura et al., 1994). Thus, 65% of LSO neurons

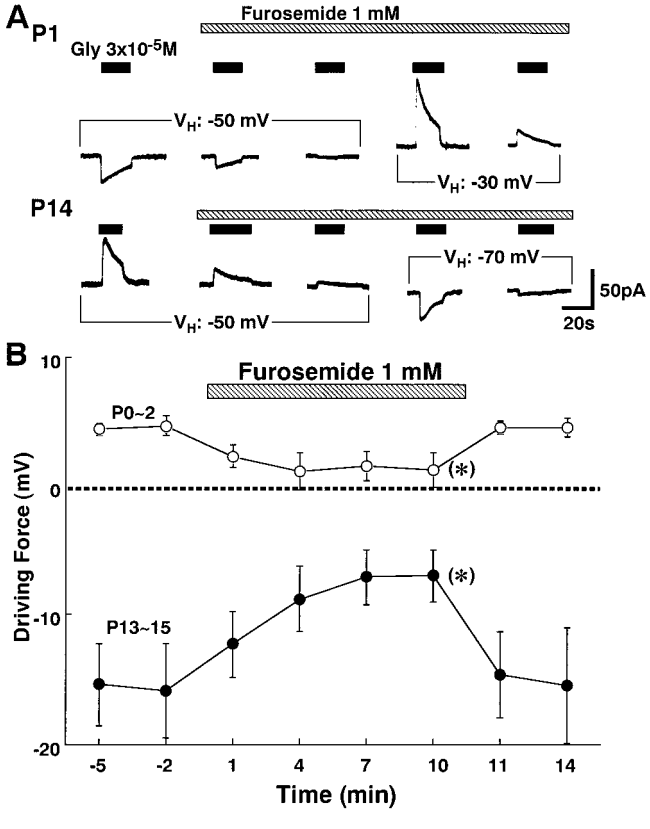

Figure 4. Effects of furosemide on E_{Gly} at two different ages. *A*, Changes in I_{Gly}s during application of 1 mM furosemide (*shaded bar*) at P1 (*top trace*) and P14 (*bottom trace*). In all following experiments, glycine was applied at an interval of 3 min (*closed bars*). The amplitude of inward (P0) and outward I_{Gly}s (P14) became smaller at a V_H of −50 mV. A shift of V_H from −50 to −30 mV at P1 (*top trace*) or to −70 mV at P14 (*bottom trace*) allowed the reappearance of I_{Gly}s. However, the amplitude of the reappeared I_{Gly}s also decreased in both neurons. *B*, Changes in the driving force (E_{Gly}–V_H) for the glycine response are plotted as a function of time before, during, and after application of 1 mM furosemide. Data are the mean ± SEM of four to six neurons at each age. *Significant difference in driving force between just before (−2 min) and during (10 min) the application of furosemide at each age ($p < 0.01$; paired *t* test).

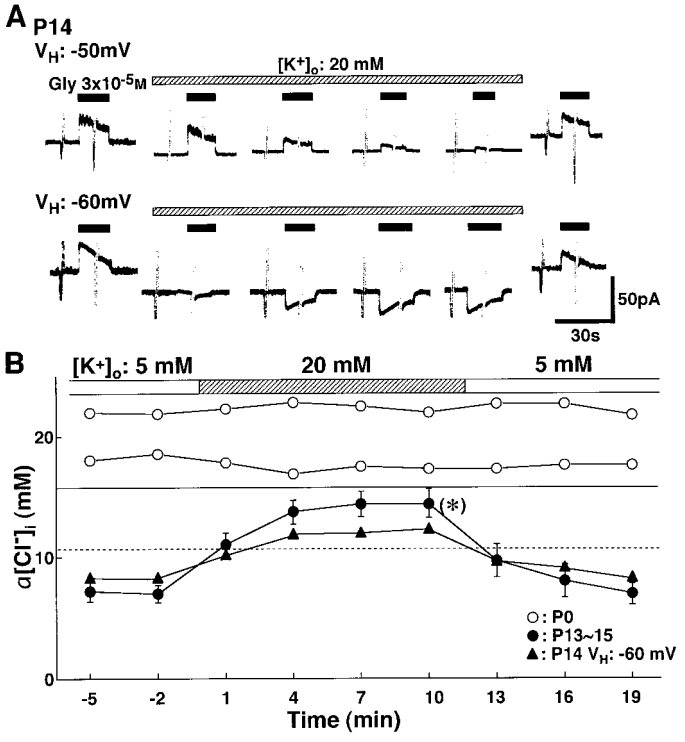

Figure 5. Effects of extracellular K^+ concentration ($[K^+]_o$) on $[Cl^-]_i$ regulation. *A*, An increase in $[K^+]_o$ from 5 to 20 mM (*shaded bar*) shifted the base current to inward direction and gradually decreased the amplitude of the outward I_{Gly} at V_Hs of −50 mV (*top trace*) and −60 mV (*bottom trace*). At V_H of −60 mV, the direction of I_{Gly} turned inward, but the amplitude was stabilized later. After reversal of $[K^+]_o$ from 20 to 5 mM, the level of base current and outward I_{Gly} recovered. *B*, Changes in α$[Cl^-]_i$ calculated from the Nernst equation using E_{Gly} and α$[Cl^-]_o$ (Table 1) were plotted as a function of time. *Solid* and *dashed horizontal lines* indicate the values of passive α$[Cl^-]_i$ calculated from the Nernst equation using α$[Cl^-]_o$ and a V_H of −50 mV (16.8 mM in 20 mM $[K^+]_o$) and −60 mV (11.3 mM in 20 mM $[K^+]_o$), respectively. Note that at P14, α$[Cl^-]_i$ in 20 mM $[K^+]_o$ at V_H of −60 mV (*closed triangles*) exceeded the passive α$[Cl^-]_i$ (*dashed line*). Two representative examples of α$[Cl^-]_i$ at P0 (*open circles*) were less influenced by 20 mM $[K^+]_o$ ($n = 4$). *Closed circles*, Mean ± SEM of four neurons at P13–P15. Other symbols show the data of each neuron. *Significant difference in α$[Cl^-]_i$ between just before (−2 min) and during (10 min) the application of 20 mM $[K^+]_o$ ($p < 0.01$; paired *t* test).

with glycine-induced depolarizing responses at P0–P2 may reflect an inherent variability within the LSO.

Possible mechanisms involved in regulation of $[Cl^-]_i$

In our studies, $[Cl^-]_i$ decreased markedly between P6–P8 and P13–P15, suggesting a change in the regulatory mechanisms of $[Cl^-]_i$ during this period. Cl^-–ATPase, KCC, NKCC, Cl^-–HCO_3^- exchange and Na^+-dependent Cl^-–HCO_3^- exchange have been implicated in the regulation of $[Cl^-]_i$ in neurons (Kaila, 1994). However, others suggest that Cl^-–HCO_3^- exchange and Na^+-dependent Cl^-–HCO_3^- exchange contribute minimally to $[Cl^-]_i$ regulation (Ballanyi and Grafe, 1985; Thompson et al., 1988). Furthermore, because we used HEPES-buffered solutions without HCO_3^-, Cl^-–HCO_3^- exchange and Na^+-dependent Cl^-–HCO_3^- exchange are likely to be negligible in the present study. Cl^-–ATPase is classified as a primary active Cl^- transport system driven directly by the consumption of ATP (Inagaki et al., 1996). However, there is little information regarding Cl^-–ATPase in neurons (Kaila, 1994). Ethacrynic acid, which inhibits Cl^-–ATPase (Shiroya et al., 1989), was applied to LSO neurons in a similar protocol to the furosemide work (Fig. 4) with variable effects on the glycine response (data not shown). Thus, a significant contribution of Cl^-–ATPase to the developmental regulation of $[Cl^-]_i$ could not be confirmed in the present study.

KCC (Gillen et al., 1996; Payne et al., 1996) and NKCC (Gamba et al., 1994; Payne and Forbush, 1994) have been identified. Recently, using ribonuclease protection analysis and *in situ* hybridization, the developmental increase in the cation–Cl^- cotransporters, including KCC and NKCC, was demonstrated in rat neocortex (Clayton et al., 1998). However, the functional involvement of KCC and NKCC in the regulation of $[Cl^-]_i$ in developing neurons is still unclear. To examine the functional roles of these cotransporters in regulating $[Cl^-]_i$, we used several interventions to manipulate KCC and NKCC function, e.g., furosemide and alternation of $[K^+]_o$, $[K^+]_i$, and $[Na^+]_o$. Because resting Cl^- permeability is very low in neurons (Thompson and Gähwiler, 1989), opening of Cl^- channels only allows flux based on the difference between $[Cl^-]_i$ and $[Cl^-]_o$ and the membrane potential. The inherent $[Cl^-]_i$-regulating mechanism is responsible for the recovery of $[Cl^-]_i$ to its original value.

Furosemide

Although both KCC and NKCC have different affinities to furosemide, they are almost completely inhibited by 1 mM furosemide

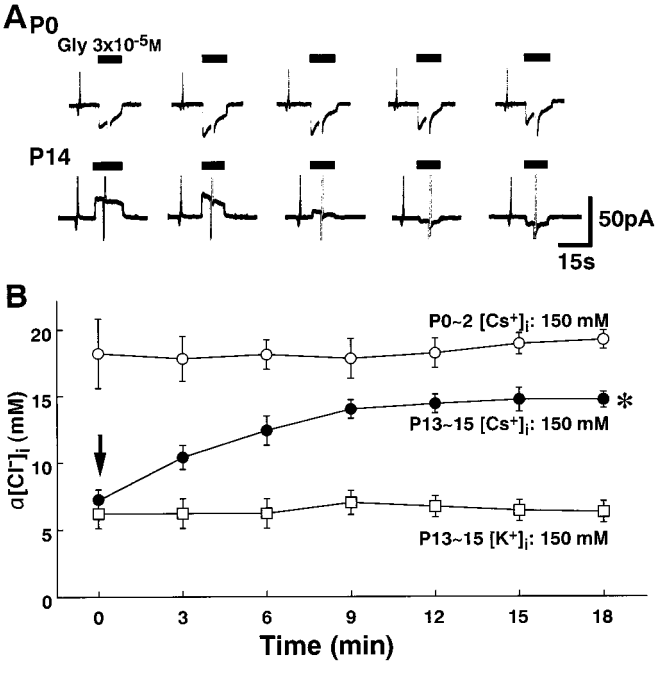

Figure 6. Effects of intracellular perfusion of Cs^+ on $[Cl^-]_i$ regulation. *A*, *Top trace*, The inward I_{Gly} could be maintained at a V_H of −50 mV in 150 mM CsCl pipette solution ($[Cs^+]_{pipette}$) at P0. *Bottom trace*, $[Cs^+]_{pipette}$ gradually decreased the amplitude of outward I_{Gly} at P14. In this neuron, the direction of I_{Gly} was finally changed to inward at a V_H of −50 mV. *B*, Changes in α$[Cl^-]_i$ were plotted as a function of time in 150 mM $[Cs^+]_{pipette}$ and 150 mM KCl pipette solution ($[K^+]_{pipette}$). Note that α$[Cl^-]_i$ in the $[Cs^+]_{pipette}$ obtained at the first application of glycine was almost equal to that in $[K^+]_{pipette}$ at P13–P15 (*arrow*). However, α$[Cl^-]_i$ in the $[Cs^+]_{pipette}$ gradually increased at P13–P15. Data represent the mean ± SEM of four to five neurons in each condition. *α$[Cl^-]_i$ after the seventh application of glycine (18 min) was significantly higher than the control (0 min) in P13–P15 LSO neurons in the $[Cs^+]_{pipette}$ ($p < 0.01$; paired *t* test).

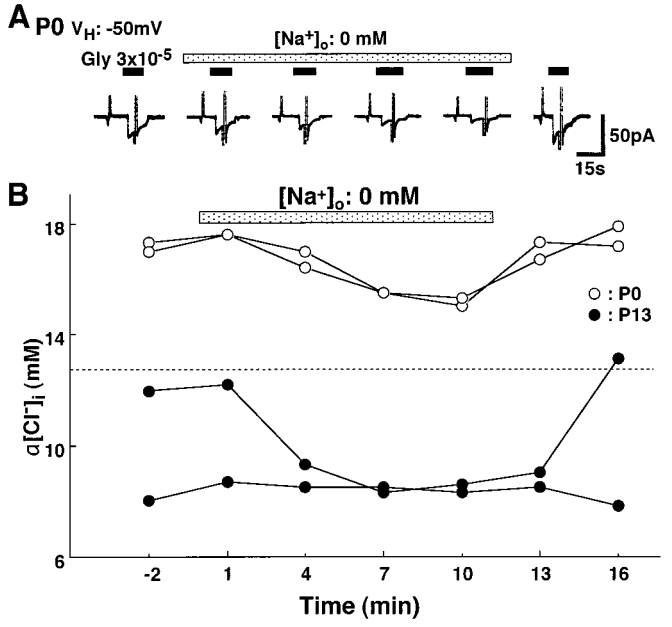

Figure 7. Effects of extracellular Na^+ concentration ($[Na^+]_o$) on $[Cl^-]_i$ regulation. *A*, At P0, glycine (*closed bars*) induced an inward current at V_H of −50 mV in the modified standard solution (Table 1). A change of $[Na^+]_o$ from 110 to 0 mM (*dotted bar*) resulted in a gradual reduction of inward I_{Gly}. Reversal of $[Na^+]_o$ to 110 mM resulted in the return of amplitude of I_{Gly} to basal levels. *B*, Changes in α$[Cl^-]_i$ were plotted as a function of time. In both two neurons at P0 (*opened circles*), α$[Cl^-]_i$ gradually decreased in the absence of $[Na^+]_o$. On the other hand, the effect of 0 mM $[Na^+]_o$ on α$[Cl^-]_i$ varied at P13 (n = 4). Two representative examples at P13–P15 showing the most and least affected neurons by 0 mM $[Na^+]_o$ (*closed circles*).

(Gillen et al., 1996). In the presence of 1 mM furosemide, repetitive application of glycine gradually decreased the amplitude of I_{Gly}s and brought E_{Gly}s close to V_H both at P0–P2 and P13–P15 (Fig. 4). However, furosemide never reversed the polarity of I_{Gly}, indicating that in the presence of furosemide, α$[Cl^-]_i$ in LSO neurons seems to be passively determined by V_H and α$[Cl^-]_o$ irrespective of developmental age. The results suggest that the furosemide-sensitive mechanisms, such as NKCC in immature and KCC in mature, play a substantial role in the maintenance of $[Cl^-]_i$ in both ages.

Effect of $[K^+]_i$, $[K^+]_o$, and $[Na^+]_o$ on regulating $[Cl^-]_i$

To evaluate the contribution of furosemide-sensitive Cl^- extrusion mechanism to lower $[Cl^-]_i$ in LSO neurons, we used the following two methods: (1) increases in $[K^+]_o$, and (2) substitution of $[Cs^+]_i$ for $[K^+]_i$. In high $[K^+]_o$, α$[Cl^-]_i$ gradually increased in LSO neurons at P13∼P15 (Fig. 5). The gradual increase of $[Cl^-]_i$ in $[Cs^+]_{pipette}$ was observed at P13∼P15 (Fig. 6), which is consistent with the results of previous studies demonstrating that E_{GABA} and E_{IPSP} with Cs^+-filled microelectrodes are generally less negative than those with K^+-filled electrodes in adult CA3 hippocampal neurons (Thompson and Gähwiler, 1989). In the experiments with high $[K^+]_o$ and the use of $[Cs^+]_{pipette}$ at P13∼P15, the glycine responses often reversed their polarities unlike furosemide (Figs. 5*A*, 6*A*, *bottom trace*). Together these results indicate that the direction of furosemide-sensitive Cl^- extrusion mechanism is independent of V_H and determined by K^+ gradient. On the other hand, high $[K^+]_o$ and $[Cs^+]_{pipette}$ did not affect I_{Gly} and α$[Cl^-]_i$ in immature LSO neurons (Figs. 5*B*, 6*B*, *open circles*). These findings suggest that the K^+ gradient-sensitive Cl^- extrusion mechanism is not well developed in immature LSO neurons. Indeed, the amplitude of the outward I_{Gly} decreased at a V_H of −30 mV in immature neurons in which inward I_{Gly} at a V_H of −50 mV was well maintained (Fig. 8). These are agreeing that KCC2 expression appears perinatally and increases dramatically after the first week of postnatal life (Clayton et al., 1998).

NKCC catalyzes an electroneutral Cl^- uptake (Kaila, 1994) and has been identified in CNS neurons (Misgeld et al., 1986; Rohrbough and Spitzer, 1996; Plotkin et al., 1997; Clayton et al., 1998). Therefore, NKCC is a possible candidate transporter that promotes accumulation of Cl^- into the cell and whose activity is regulated by the Na^+-gradient (Ballanyi and Grafe, 1985). Indeed, displacement of $[Na^+]_o$ with NMDG decreased α$[Cl^-]_i$ in all immature LSO neurons (Fig. 7), in which Na^+-dependent mechanisms such as NKCC were preferentially blocked because of the disappearance of Na^+ in both sides. In addition, although the constant inward I_{Gly} was well maintained at a V_H of −50 mV at P0, the outward I_{Gly} at a V_H of −30 mV became less evident and finally almost null (Fig. 8). The possible explanations for the maintenance of Cl^- accumulation at a V_H of −50 mV and the disappearance of Cl^- accumulation at a V_H of −30 mV in immature LSO neurons are: (1) a flux of Cl^- through glycine-

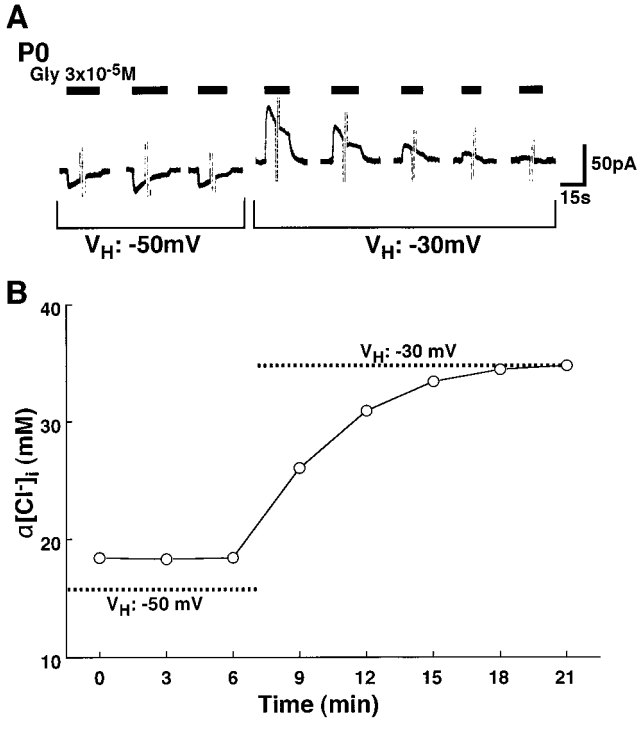

Figure 8. Effect of V_H on $[Cl^-]_i$ regulation in an immature LSO neuron. *A*, At P0, glycine (*closed bars*) induced a constant amplitude of inward I_{Gly} at a V_H of −50 mV in a standard extracellular solution and 150 mM $[K^+]_{pipette}$. A shift of V_H from −50 (*left*) to −30 mV (*right*) altered the direction of I_{Gly} to outward. The amplitude of the outward I_{Gly} gradually decreased and finally became almost null. *B*, Changes in α$[Cl^-]_i$ in the same neuron shown in *A* were plotted as a function of time (*opened circles*). *Dashed lines* indicate passive α$[Cl^-]_i$s calculated from the Nernst equation using α$[Cl^-]_o$ in the standard extracellular solution and the value of V_H, where passive α$[Cl^-]_i$s are 15.7 mM and 34.8 mM at V_H of −50 and −30 mV, respectively. Note that although α$[Cl^-]_i$ could be maintained greater than the passive α$[Cl^-]_i$ at a V_H of −50 mV, it was not lower than the passive α$[Cl^-]_i$ at a V_H of −30 mV.

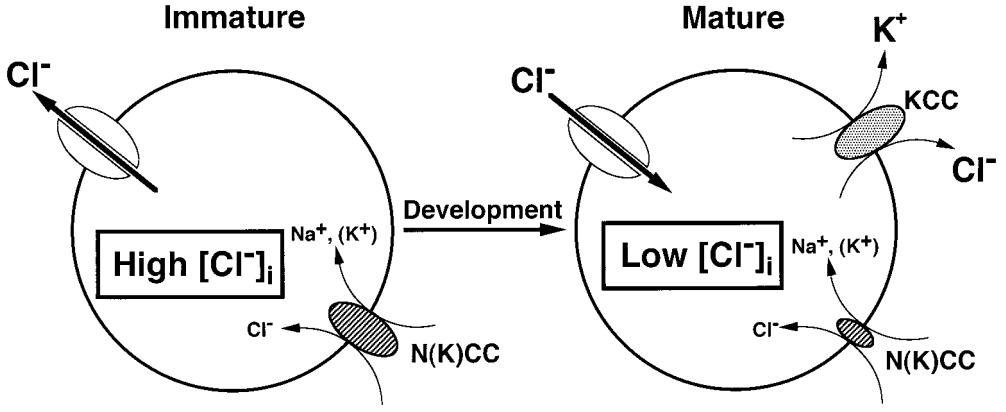

Figure 9. A schematic illustration of the possible model involved in the regulation of $[Cl^-]_i$ by cotransporters in developing LSO neurons. The function of NKCC, furosemide, and $[Na^+]_o$-sensitive inward Cl^- cotransporter decreases with age. KCC, a furosemide-sensitive outward Cl^- cotransporter, is only represented in mature LSO neurons. *Thick arrows* in immature and mature LSO neurons indicate the direction of Cl^- ion flux through the Cl^- channels.

operated Cl^- channels reduces the electrochemical gradients of Cl^- at any V_Hs, but $[Cl^-]_i$ attained after the application of glycine varies with V_H. In the LSO neuron shown in Figure 8, glycine induced an efflux of Cl^- at a V_H of −50 mV, which could decrease $[Cl^-]_i$, resulting in increasing a difference between $[Cl^-]_i$ and $[Cl^-]_o$ (Cl^- chemical gradient) and thus increasing a driving force for inwardly directed NKCC. On the contrary, an influx of Cl^- by glycine at a V_H of −30 mV increased $[Cl^-]_i$, resulting in reducing a Cl^- chemical gradient and decreasing a driving force for inwardly directed NKCC. Thus, Cl^- accumulation adding to the passive $\alpha[Cl^-]_i$ by inward NKCC might not be evident in function at a V_H of −30 mV in the LSO neuron shown in Figure 8; and (2) voltage dependency of NKCC function could not be ruled out in the present study.

On the other hand, $[Na^+]_o$-dependent accumulation varied at P13–P15. This is compatible with the report that mRNA for NKCC1 (BSC2) shows a transient peak at early stages of development but gradually declines with age in the rat brain (Plotkin et al., 1997). Recent report demonstrates that $[Cl^-]_i$ is passively increased by coincident membrane depolarization simultaneous with activation of glycine-operated Cl^- channels in immature LSO neurons (Backus et al., 1998). In our present study, however, $[Cl^-]_i$ was well maintained even at a V_H of −50 mV in immature neurons. Thus, our data clearly indicate that genetically programmed changes of $[Cl^-]_i$ regulation occur during fetal and postnatal LSO neurons.

In summary, our results indicate that in LSO neurons, (1) $[Cl^-]_i$ is mainly determined by a net flux mediated by furosemide-sensitive mechanism, i.e., KCC and NKCC, (2) high $[Cl^-]_i$ in immature neurons is caused by the presence of functional Na^+-dependent cotransporter, i.e., NKCC and lack of K^+-dependent cotransporter, i.e., KCC, and (3) with maturity, higher activity of K^+-dependent Cl^- extrusion relative to Na^+-dependent Cl^- accumulation maintains $[Cl^-]_i$ at low levels (Fig. 9).

Functional implications of glycinergic inputs in developing LSO neurons

The probability of firing action potentials in LSO neurons depends on the timing differences of arrival from the contralateral (glycinergic) and ipsilateral (glutamatergic) inputs, a process that encodes differences in interaural intensity and supplies the chief cues to localize sounds in space (Wu and Kelly, 1992; Thomas et al., 1996). Our present results suggest that there is a critical transition in cotransporters, which occurs between P6–P8 and P13–P15. As a result, $[Cl^-]_i$ decreases and glycine responses switch from depolarization to the adult pattern of hyperpolarization. This transition occurs during a period at which previous studies indicate that physiological hearing in rats and gerbils begins (P12–P14; Sanes and Rubel, 1988; Kandler and Friauf, 1995). However, the physiological development of LSO neurons occurs even in the absence of hearing experience (Kandler and Friauf, 1995). The influence of hearing experience and synaptic activity to LSO in controlling Cl^- transport remains to be elucidated.

GABA and glycine act neurotrophically in immature neurons (Ikeda et al., 1997; Flint et al., 1998; Kirsch and Betz, 1998). Glycine-induced depolarization might increase $[Ca^{2+}]_i$ through voltage-dependent Ca^{2+} channels and NMDA channels in the LSO similar to its effects in other CNS areas during development (LoTurco et al., 1995; Leinekugel et al., 1997; Obrietan and van den Pol, 1997; Flint et al., 1998). Removal of glycinergic inputs in LSO neurons in immature animals by cochlea ablation or chronic strychnine application leads to a hypertrophic response in the shape and length of their dendrites (Sanes and Chokshi, 1992) and causes a depolarizing shift in IPSP reversal potential (Kotak and Sanes, 1996). Thus, glycinergic depolarization may play an important role in the development and refinement of LSO neurons. The appropriate timing of changes in Cl^- transport with achieving neuronal maturity assumes that glycinergic input will be inhibitory and thus help mediate interaural intensity comparisons.

REFERENCES

Akaike N (1997) Gramicidin perforated patch recording and intracellular chloride activity in excitable cells. Prog Biophys Mol Biol 65:251–264.

Akaike N, Harata N (1994) Nystatin perforated patch recording and its applications to analyses of intracellular mechanisms. Jpn J Physiol 44:433–473.

Alvarez-Leefmans FJ (1990) Intracellular Cl^- regulation and synaptic inhibition in vertebrate and invertebrate neurons. In: Chloride channels and carriers in nerve, muscle and glial cells (Alvarez-Leefmans FJ, Russel JM, eds), pp 109–158. New York: Plenum.

Backus KH, Deitmer JW, Friauf E (1998) Glycine-activated currents are changed by coincident membrane depolarization in developing rat auditory brainstem neurones. J Physiol (Lond) 507:783–794.

Ballanyi K, Grafe P (1985) An intracellular analysis of γ-aminobutyric-acid-associated ion movements in rat sympathetic neurones. J Physiol (Lond) 365:41–58.

Chen G, Trombley PQ, van den Pol AN (1996) Excitatory actions of GABA in developing rat hypothalamic neurones. J Physiol (Lond) 494:451–464.

Clayton GH, Owens GC, Wolff JS, Smith RL (1998) Ontogeny of cation-Cl^- cotransporter expression in rat neocortex. Brain Res Dev Brain Res 109:281–292.

Ebihara S, Shirato K, Harata N, Akaike N (1995) Gramicidin-perforated patch recording: GABA response in mammalian neurones with intact intracellular chloride. J Physiol (Lond) 484:77–86.

Flint AC, Liu X, Kriegstein AR (1998) Nonsynaptic glycine receptor activation during early neocortical development. Neuron 20:43–53.

Gamba G, Miyanoshita A, Lombardi M, Lytton J, Lee WS, Hediger MA, Hebert SC (1994) Molecular cloning, primary structure, and characterization of two members of the mammalian electroneutral sodium-(potassium)-chloride cotransporter family expressed in kidney. J Biol Chem 269:17713–17722.

Gillen CM, Brill S, Payne JA, Forbush III B (1996) Molecular cloning and functional expression of the K-Cl cotransporter from rabbit, rat and human. A new member of the cation-chloride cotransporter family. J Biol Chem 271:16237–16244.

Haas M (1994) The Na-K-Cl cotransporters. Am J Physiol 267: C869–C885.

Ikeda Y, Nishiyama N, Saito H, Katsuki H (1997) $GABA_A$ receptor stimulation promotes survival of embryonic rat striatal neurons in culture. Brain Res Dev Brain Res 98:253–258.

Inagaki C, Hara M, Zeng X (1996) A Cl^- pump in rat brain neurons. J Exp Zool 275:262–268.

Kaila K (1994) Ionic basis of $GABA_A$ receptor channel function in the nervous system. Prog Neurobiol 42:489–537.

Kaila K, Lamsa K, Smirnov S, Taira T, Voipio J (1997) Long-lasting GABA-mediated depolarization evoked by high frequency stimulation in pyramidal neurons of rat hippocampal slice is attributable to a network-driven, bicarbonate-dependent K^+ transient. J Neurosci 17:7662–7672.

Kandler K, Friauf E (1995) Development of glycinergic and glutamatergic synaptic transmission in the auditory brainstem of perinatal rats. J Neurosci 15:6890–6904.

Kirsch J, Betz H (1998) Glycine-receptor activation is required for receptor clustering in spinal neurons. Nature 392:717–720.

Komune S, Nakagawa T, Hisashi K, Kimitsuki T, Uemura T (1993) Mechanism of lack of development of negative endocochlear potential in guinea pigs with hair cell loss. Hear Res 70:197–204.

Korpi ER, Luddens H (1997) Furosemide interactions with brain $GABA_A$ receptors. Br J Pharmacol 120:741–748.

Kotak VC, Sanes DH (1995) Synaptically evoked prolonged depolarizations in the developing auditory system. J Neurophysiol 74:1611–1620.

Kotak VC, Sanes DH (1996) Developmental influence of glycinergic transmission: regulation of NMDA receptor-mediated EPSPs. J Neurosci 16:1836–1843.

Leinekugel X, Medina I, Khalilov I, Ben-Ari Y, Khazipov R (1997) Ca^{2+} oscillations mediated by the synergistic excitatory actions of $GABA_A$ and NMDA receptors in the neonatal hippocampus. Neuron 18:243–255.

LoTurco JJ, Owens DF, Heath MJ, Davis MB, Kriegstein AR (1995) GABA and glutamate depolarize cortical progenitor cells and inhibit DNA synthesis. Neuron 15:1287–1298.

Luhmann HJ, Prince DA (1991) Postnatal maturation of the GABAergic system in rat neocortex. J Neurophysiol 65:247–263.

McCormick DA, Prince DA (1987) Post-natal development of electrophysiological properties of rat cerebral cortical pyramidal neurones. J Physiol (Lond) 393:743–762.

Misgeld U, Deisz RA, Dodt HU, Lux HD (1986) The role of chloride transport in postsynaptic inhibition of hippocampal neurons. Science 232:1413–1415.

Nabekura J, Kawamoto I, Akaike N (1994) Developmental change in voltage dependency of NMDA receptor-mediated response in nucleus tractus solitarii neurons. Brain Res 648:152–156.

Nakagawa T, Shirasaki T, Wakamori M, Fukuda A, Akaike N (1990) Excitatory amino acid response in isolated nucleus tractus solitarii neurons of the rat. Neurosci Res 8:114–123.

Obrietan K, van den Pol AN (1997) GABA activity mediating cytosolic Ca^{2+} rises in developing neurons is modulated by cAMP-dependent signal transduction. J Neurosci 17:4785–4799.

Payne JA, Forbush III B (1994) Alternatively spliced isoforms of the putative renal Na-K-Cl cotransporter are differentially distributed within the rabbit kidney. Proc Natl Acad Sci USA 91:4544–4548.

Payne JA, Stevenson TJ, Donaldson LF (1996) Molecular characterization of a putative K-Cl cotransporter in rat brain. J Biol Chem 271:16245–16252.

Plotkin MD, Snyder EY, Hebert SC, Delpire E (1997) Expression of the Na-K-2Cl cotransporter is developmentally regulated in postnatal rat brains: a possible mechanism underlying GABA's excitatory role in immature brain. J Neurobiol 33:781–795.

Rhee JS, Ebihara S, Akaike N (1994) Gramicidin perforated patch-clamp technique reveals glycine-gated outward chloride current in dissociated nucleus solitarii neurons of the rat. J Neurophysiol 72:1103–1108.

Rohrbough J, Spitzer NC (1996) Regulation of intracellular Cl^- levels by Na^+-dependent Cl^- cotransport distinguishes depolarizing from hyperpolarizing $GABA_A$ receptor-mediated responses in spinal neurons. J Neurosci 16:82–91.

Sanes DH (1993) The development of synaptic function and integration in the central auditory system. J Neurosci 13:2627–2637.

Sanes DH, Chokshi P (1992) Glycinergic transmission influences the development of dendrite shape. NeuroReport 3:323–326.

Sanes DH, Rubel EW (1988) The ontogeny of inhibition and excitation in the gerbil lateral superior olive. J Neurosci 8:682–700.

Shiroya T, Fukunaga R, Akashi K, Shimada N, Takagi Y, Nishino T, Hara M, Inagaki C (1989) An ATP-driven Cl^- pump in the brain. J Biol Chem 264:17416–17421.

Staley KJ, Soldo BL, Proctor WR (1995) Ionic mechanisms of neuronal excitation by inhibitory $GABA_A$ receptors. Science 269:977–981.

Suneja SK, Benson CG, Gross J, Potashner SJ (1995) Evidence for Glutamatergic projections from the cochlear nucleus to the superior olive and the ventral nucleus of the lateral lemniscus. J Neurochem 64:161–171.

Thompson SM, Gähwiler BH (1989) Activity-dependent disinhibition. II. Effects of extracellular potassium, furosemide, and membrane potential on ECl- in hippocampal CA3 neurons. J Neurophysiol 61:512–523.

Thompson SM, Deisz RA, Prince DA (1988) Outward chloride/cation co-transport in mammalian cortical neurons. Neurosci Lett 89:49–54.

Wu SH, Kelly JB (1992) Binaural interaction in the lateral superior olive: time difference sensitivity studied in mouse brain slice. J Neurophysiol 68:1151–1159.

Zhang L, Spigelman I, Carlen PL (1991) Development of GABA-mediated, chloride-dependent inhibition in CA1 pyramidal neurones of immature rat hippocampal slices. J Physiol (Lond) 444:25–49.